Clay Minerals, (2017) **52**, 275–297

Nature, genesis and industrial properties of the kaolin from Masirah Island, Oman

BERNHARD PRACEJUS[1], IFTIKHAR AHMED ABBASI[1,*], SALAH AL-KHIRBASH[1] AND MOHAMMAD AL-AAMRI[2]

[1] *Earth Science Department, College of Science, Sultan Qaboos University, Muscat, Oman*
[2] *Public Authority for Craft Industry, Muscat, Oman*

(*Received 8 December 2016; revised 5 August 2017; Editor: George Christidis*)

ABSTRACT: Kaolin deposits >10 m thick overlie unconformably a Mesozoic ophiolite sequence at Jabal Humr, Masirah Island, Oman. The clay's mineralogical and chemical composition, plasticity and moisture content were measured to determine its genesis and suitability for commercial usage. The clay-rich raw material contains 76–94% kaolinite and varying amounts of quartz (micro sheets coating kaolinite) and calcite as well as secondary sulfates. The mode of occurrence, an associated shallow-marine iron oolite/pisolite unit, various secondary minerals which can only form in a gossan environment (oxidation zone of a much older sulfide deposit), and minerals such as gypsum that are highly unstable within a laterite, have led to the conclusion that the Jabal Humr kaolinite deposit cannot have the lateritic origin that has been suggested previously. Rather, it must have formed in a coastal marine environment with a subsequent strong geochemical overprint from the underlying gossan environment, after being enveloped by Tertiary carbonates. A high plasticity and its light colour after firing indicate that this material is suitable for industrial use, especially in pottery. Occasional high contents of up to ~25% extremely fine-grained quartz (sheet-like, <50 nm thick) reduce the need for quartz addition during the processing for ceramic materials; such natural kaolinite-quartz mixtures already produce a suitable blend of materials. The possible occurrence of spalling during or after firing, caused by the sporadic presence of accessory calcite, can be avoided by by further addition of quartz which leads to the formation of calcium silicate.

KEYWORDS: kaolinite, clay, ophiolite, Masirah Island, Oman.

The present study describes the main features of the kaolin deposit at Jabal Humr on Masirah Island (Fig. 1; 20°32′12″N; 58°52′42″E; centre of rectangular outline), to shed light on the formation of the deposit (*e.g.* possible parent rocks and overprinting), and describes the industrial properties of the raw material. Other clay exposures on the island are either mixed with abundant ferruginous material or are too small in overall size to be of any commercial significance.

* E-mail: iftikhar@squ.edu.om
https://doi.org/10.1180/claymin.2017.052.3.01

Research on Masirah kaolin is very sparse. The material has been mentioned only briefly in the description of the geological map of Oman (Peters *et al.*, 1995), where it was referred to as a lateritic material, and cited by Menkveld-Gfeller & Decrouez (2004). Laterites can form from many igneous rocks such as felsics (granites, gneisses), mafics (basalts and gabbros), alkaline rocks (phonolites, nepheline syenites) and ultramafics (peridotites, dunites, serpentinites) (Schellmann, 1986; McFarlane & Bowden, 1992; Michailidis *et al.*, 1993; Malengreau & Sposito, 1997; Bourman & Ollier, 2002).

Such lateritic products of tropical–subtropical weathering show hints of their origins in the

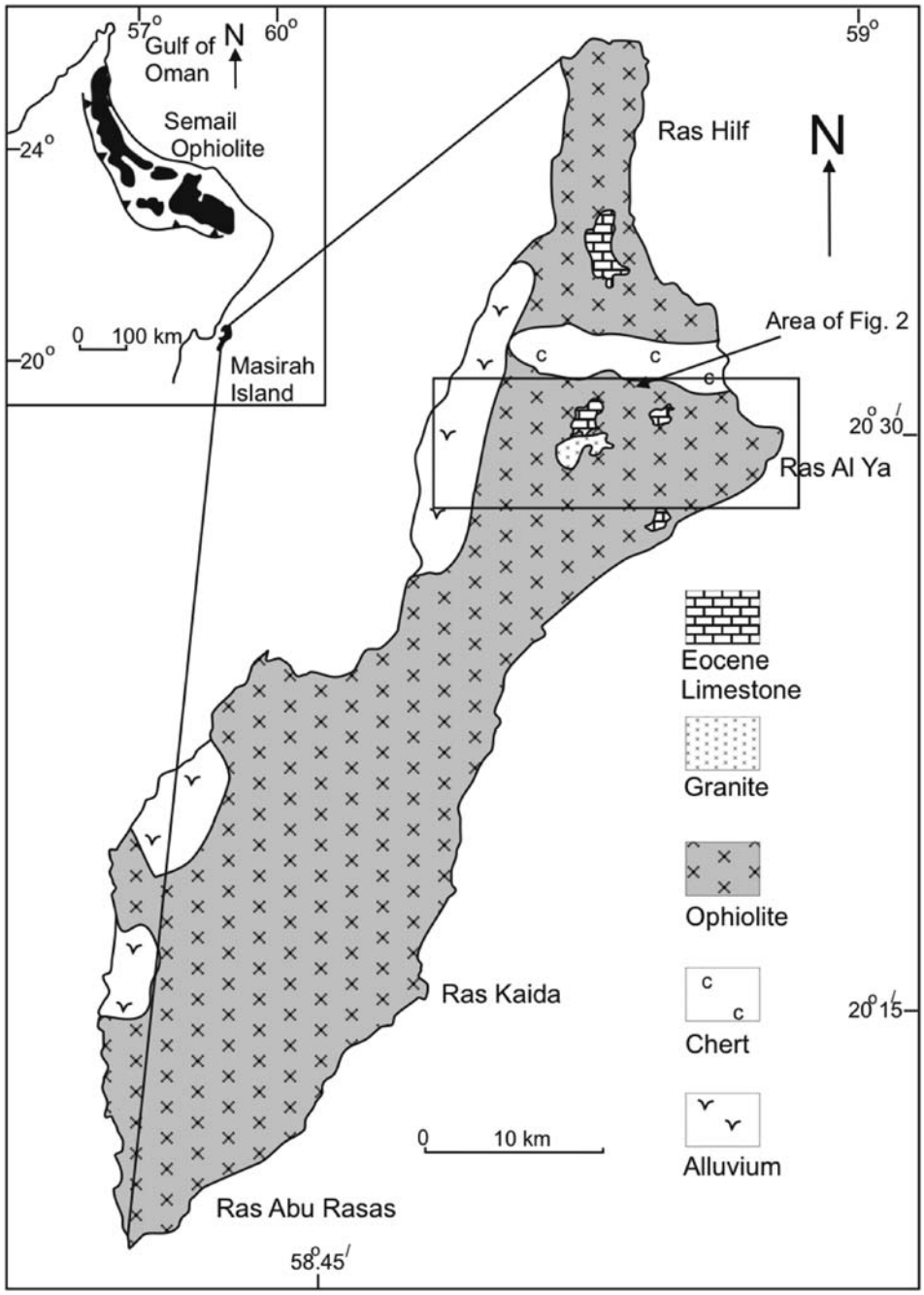

FIG. 1. Overview map of Masirah island (inset: map of Oman).

preservation of particular characteristics such as large Ni contents when being derived from ultramafics or large Al contents (gibbsite) when originating from SiO_2-poor and well drained rocks during weathering. Common to the latter is the high abundance of kaolinite and Fe oxides/oxyhydroxides (goethite, hematite),

https://doi.org/10.1180/claymin.2017.052.3.01 Published online by Cambridge University Press

giving the rock a mottled red–brown and beige–yellow appearance. The lower sections of laterites grade into the source rock, producing the so-called saprolite where Fe is less abundant. Thus, a number of criteria must be fulfilled to allow the use of the term laterite (or even saprolite for an incomplete lateritization). Although many of the igneous rocks mentioned above can be found in the vicinity of the location under investigation (granites, basalts and ultramafics), several features which are seen, or not seen, in the deposit contradict the suggestion that the Jabal Humr deposit is a laterite.

The white clay deposit (kaolinite is the major clay mineral) in the study area is part of a Tertiary sequence deposited unconformably on top of the Mesozoic Masirah ophiolite (Fig. 2a,b). The kaolin occurs between isolated Tertiary carbonate caps and the underlying ophiolitic sequence. Exposed along the northern flanks of Jabal Humr, the kaolin thins out gradually towards the south of the mountain (Ahmed *et al.*, 2014). A few other Tertiary outcrops, consisting mainly of carbonate rocks, are exposed to the east of Jabal Humr; these contain little or no kaolinite, however. Kaolin occurs sporadically in the eastern outcrops, such as at Jabal Ash Sabbah, where ~5 m of ferruginous material and altered rocks cover the underlying ophiolite. Intense oxidation occurring in the underlying rocks at Jabal Humr left its signature in the clay, as manifested by the presence of various secondary minerals. Fine-grained quartz is one of these and is significant in terms of the clay texture observed at the micro-scale, a feature that has not been observed in other kaolin deposits in Oman.

Initially, mineralogical and geochemical analyses were conducted to determine the future potential of these clays for commercial use, as well as industrial processing of the raw materials. The entire area is now under protection, however, and is no longer accessible to industry. Because early findings had already proved to be much more challenging than expected, further investigations were initiated to determine the overall nature and formation of this kaolin deposit. The physical properties, with demonstrable industrial value, had already been determined at an early research stage and are mentioned here for the sake of completeness.

GEOLOGICAL SETTING

Masirah Island, located in the Arabian Sea, is 60 km long and 20 km wide and consists of rugged hills formed of ophiolite rocks (Fig. 1). The Masirah Ophiolite nappe was obducted over the autochthonous Arabian continental margin during the Early Palaeocene (Smewing *et al.*, 1991; Peters *et al.*, 1995; Marquer *et al.*, 1998). The oceanic crust of the ophiolite sequence is only 2 km thick and was formed in Late Jurassic to Early Cretaceous times (Tithonian) during rifting between Africa and Madagascar/India (Gnos & Perrin, 1996; Immenhauser, 1996). The rifted basin was filled with pelagic sediments during the subsequent 25–30 Ma, marking quiet subsidence followed by shallow-marine platform carbonate deposition, turbidites and debris flows during the Hauterivian–Barremian (Immenhauser, 1996; Marquer *et al.*, 1998). The mid-Cretaceous also was a time of major block faulting, alkaline volcanism and intrusion of a hornblende gabbro-granite suite during the Barremian (130–125 Ma; Peters & Mercolli, 1998). One of these potassic granites intruding the ophiolite sequence is located very near Jabal Humr (Fig. 2a). These granite pods were attributed to melting of continental crust and dated at 124–146 Ma (Abbotts, 1978) which is prior to the obduction. The Late Cretaceous was the time of deposition of siliciclastic flysch and slope conglomerate. During the late Maastrichtian–early Palaeocene, intra-oceanic thrusting led to the formation of a lower and an upper Masirah nappe separated by the Main Masirah Thrust (Marquer *et al.*, 1995). This thrust event was followed by the ophiolite obduction on the Arabian continental margin during the Palaeocene.

The ophiolite sequence consists of ultramafic mantle rocks (peridotites, harzburgites) in its lowermost portion, overlain by mafic oceanic crust rocks (gabbros, basalts), which were in turn capped by sedimentary rocks (Immenhauser, 1996). On Masirah, erosion left little evidence of the mafics and the sedimentary rocks. While still under the ocean, active volcanism and associated strong faulting caused the formation of hydrothermal convection cells in the oceanic crust that yielded numerous, mostly small-scale, Cyprus-type hydrothermal Volcanogenic Massive Sulfide (VMS) deposits (Hannington *et al.*, 1998; Galley *et al.*, 2007) within the igneous rocks. Once exposed to subaerial conditions (weathering/erosion after obduction), sulfide minerals began to oxidize forming highly acidic fluids within and around the respective deposit, forming a gossan (iron cap) in at least the upper part of the orebodies (Chavéz, 2000; Essalhi *et al.*, 2011).

The kaolin from Jabal Humr has been overprinted by such acidic solutions and the corresponding high-acidity mineral development. In the Jabal Humr area,

https://doi.org/10.1180/claymin.2017.052.3.01 Published online by Cambridge University Press

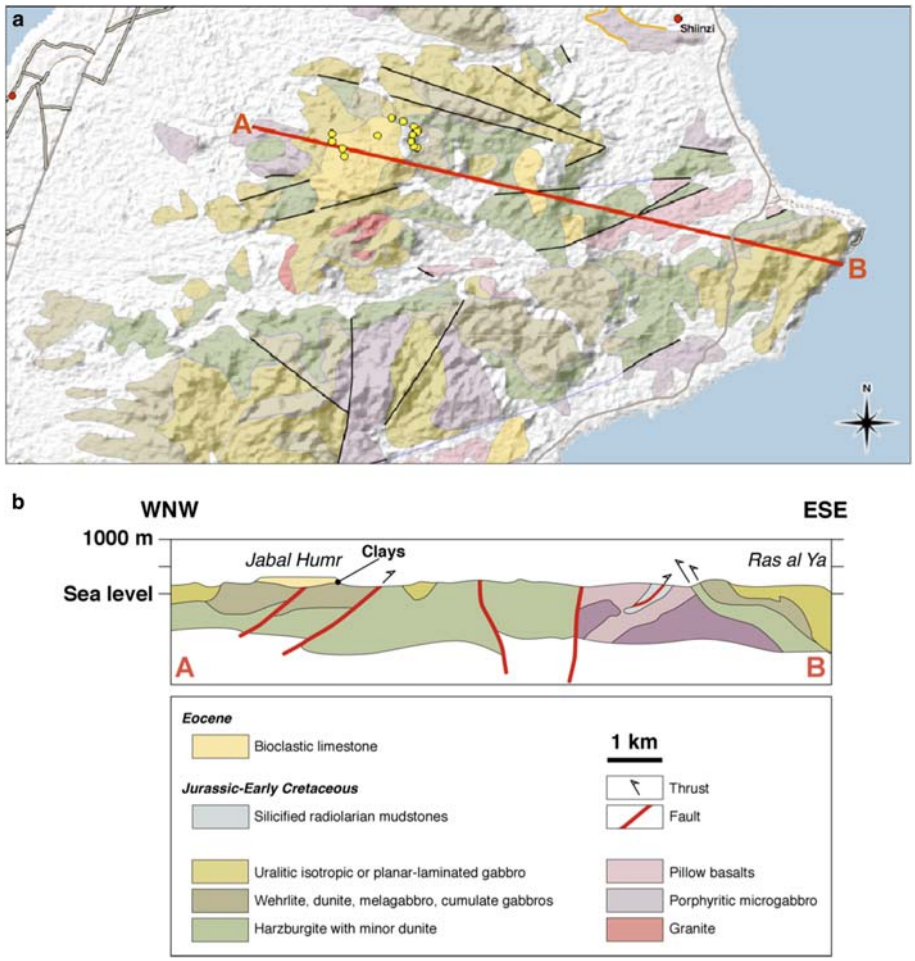

FIG. 2. (a) Geological map of Masirah. Outcrops of the clay locations are shown as yellow dots; the position of the geological profile presented in (b) is indicated by the red line from A to B; thin black and orange lines are faults; the map was produced with *SimpleDEMViewer* for Mac (version 4.4.9), ASTER GDEM data (product of METI and NASA), the geological map of Oman (Béchennec *et al.*, 1993), and QGIS (version 2.0.1-Dufour) under GNU General Public License. (b) Vertical E–W profile through the Jabal Humr area; A and B correspond to the profile line shown in part a; modified after Béchennec *et al.* (1993).

this oxidized zone was overlain by a mixed assemblage of gypsum-, quartz- and kaolinite-rich materials, which are then overlain by the main kaolin horizon some 10 m thick. A sea transgression during Middle Eocene time deposited marine carbonate sediments in the area. A Tertiary sequence, therefore, overlies unconformably the ophiolite nappes and is found at a few places, notably in Jabal Humr, Jabal Ash Sabah and Jabal Safra. Finally, all the pre-Quaternary sequences were affected by intense brittle extensional deformation leading to the present-day complex structures. Workable kaolin deposits are found only in the Jabal Humr area, where kaolin occurs below the Tertiary carbonate cap (Fig. 2b).

METHODS

Eight samples (weighing between 5 and 10 kg) were collected from the kaolin unit in the Jabal Humr area (Supplementary material Table S1, http://www.minersoc.org/pages/e_journals/dep_mat_cm.html). Representative samples were selected from the bottom

https://doi.org/10.1180/claymin.2017.052.3.01 Published online by Cambridge University Press

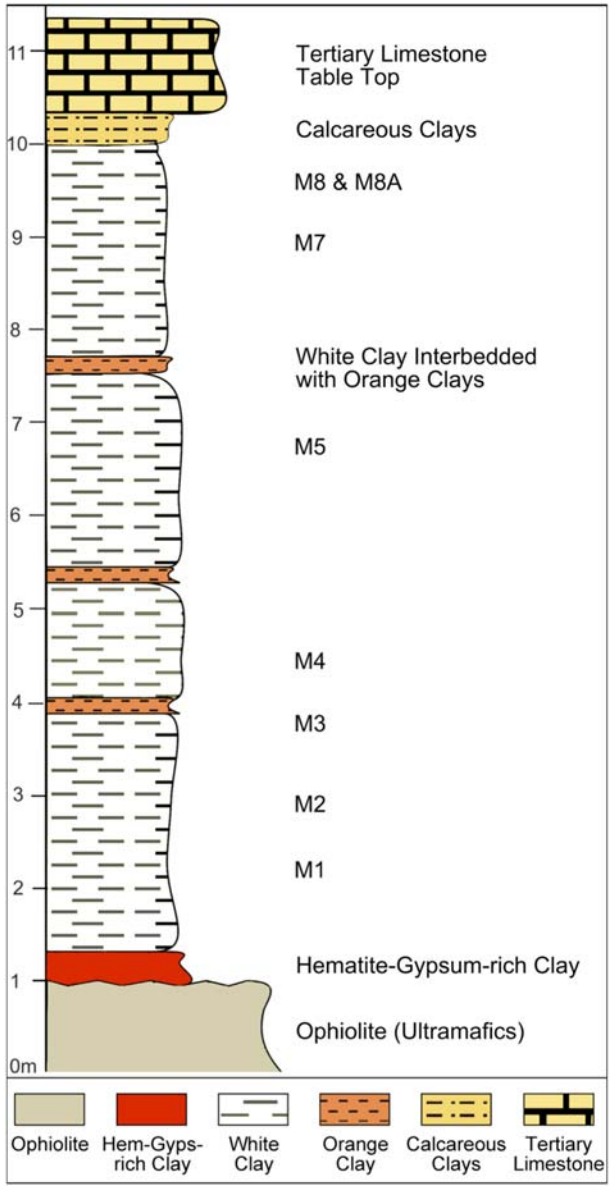

FIG. 3. Stratigraphic log of white clay in Jabal Humr, measured along the thickest clay exposure.

to the top of the clay deposit for mineralogical (X-ray diffraction, XRD) and geochemical (X-ray fluorescence, XRF) analyses and for physical tests (Plasticity – Atterberg Limits). To determine the major-element composition, the samples were analysed by XRF with a Panalytical Axios^{max} PW4400 sequential wavelength-dispersive X-ray fluorescence spectrometer, using a Rhodium target X-ray tube, excitation voltage of 25 kV and operating current of 160 mA. Trace elements were determined using a hand-held Niton XL3 XRF spectrometer.

After drying at 40°C for 24 h the kaolinite-rich samples were ground to <10 μm for study by XRD. The samples were not centrifuged or sedimented in Atterberg cylinders and were not treated with distilled water or ethylene glycol to avoid possible removal of

https://doi.org/10.1180/claymin.2017.052.3.01 Published online by Cambridge University Press

FIG. 4. (a) Photo of the outcropping kaolinite deposit below the Jabal Humr table top mountain; (b) kaolinite sampling site, the deposit is partially covered by limestone scree.

soluble components (*e.g.* metal salts). X-ray diffraction analysis was performed with an X-Pert PRO X-ray diffractometer equipped with an XCelerator using Cu-*K*α radiation (1.54060 Å, 45 kV, 40 mA). The whole-rock samples were analysed over an angular range of 5–70°2θ using a sample spinner to reduce preferred-orientation effects. Diffraction patterns were acquired using the X-Pert Data Collector software and processed manually using the "High Score Plus" software. Applying a semi-quantitative approach for determining mineral abundances, the main kaolinite and quartz peaks were used to estimate their respective concentrations. All samples were examined initially as raw materials and after firing at 900 and 1040°C in a kiln at Bahla Clay Factory to study their suitability for ceramics purposes. The plastic and liquid limits (Atterberg Limits) of the samples were determined according to the British Standards BS-1377 (1975). Drying and firing shrinkage were determined for kaolinite paste moulds heated at 900–1040°C at Bahla ceramic factory.

RESULTS

Stratigraphy

Greyish white to buff-coloured kaolinitic clay occurs in Jabal Humr area at 20°32′11.6″N 58°52′ 41″E (Fig. 2a,b). The clay sequence with a maximum thickness of ~10 m, was deposited on top of the eroded Mesozoic Masirah ophiolite sequence, and is overlain by an almost horizontal Tertiary carbonate table-top of the Jabal Humr mountain (Fig. 3). The deposit crops out with varying thickness along the northern and northwestern side of the mountain. Most parts of the clay exposure are covered with scree (Fig. 4a,b), but are accessible along the ridge. At 20°32′06″N and 58°51′ 46″E on the western side of the mountain, 1–2 m thick clay is exposed along very large downthrown blocks, possibly along a major landslide. The homogeneous kaolin beds are separated by 10–20 cm-thick layers of orange clays (Fig. 3) which contain Fe oxides/ oxyhydroxides and gypsum, while halite appears in varying amounts in all units. Near the contact with the underlying ophiolite, red hematitic and gypsum-rich kaolin materials mark the base of the kaolin sequence with minerals derived from the oxidation/breakdown of sulfides in the ophiolite (gossan environment), while the uppermost part of the sequence is defined by ~1 m-thick calcareous kaolinitic clays which grade into the overlying carbonate rocks (Fig. 3). The orange clays may also represent oxidation fronts moving upwards through capillary forces. About 1 km west of the Jabal Humr outcrops, alkali granite dykes appear over a large area (Figs 5 and 6a,b).

Clay textures and intergrowths

Under the scanning electron microscope (SEM), the samples display some unusual features (Fig. 7a–d):

- When viewed perpendicular to the bedding of the clay, a strong undulating texture is apparent throughout the sample which cannot be explained either by normal sedimentation or by *in situ* formation of the clays (Fig. 7a).

https://doi.org/10.1180/claymin.2017.052.3.01 Published online by Cambridge University Press

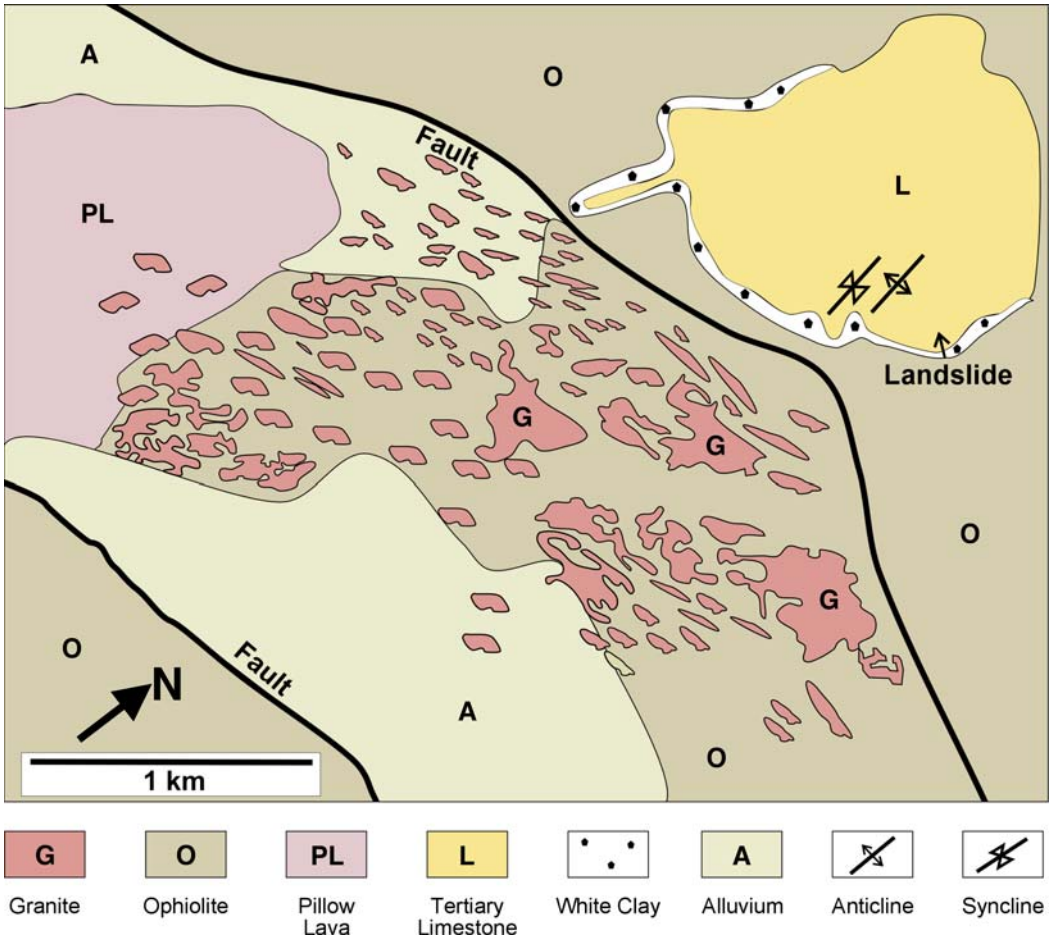

FIG. 5. Detailed geological outcrop map of K-granite bodies in close association with the white clays (Abbotts, 1978).

- Viewing the top of individual layers, euhedral thin platelets are stacked on top of each other; the typical thick stacks or vermiform kaolinite aggregates are absent (Fig. 7b).
- Between kaolin layers, the finest films of amorphous, SiO_2, confirmed by energy dispersive (EDS) spot analysis, display fine dehydration-like cracks at high magnification (Fig. 7c, d), resembling fine opal-CT coatings. Siliceous micro-fossils that could have acted as a source for (remobilized?) SiO_2 or detrital quartz grains were not detected in any of the samples examined.

As for many other geological materials in Oman, the finest of halite (NaCl) crystal aggregates occasionally impregnate the clay and are discerned readily by their cubic habit.

Mineralogy of clay materials

The major-mineral composition of the clay-rich materials varies between the limits displayed by the two representative XRD traces of the Masirah samples (Table 1 Fig. 8a). Occasionally, goethite becomes a major constituent, while anatase (TiO_2) and halite are present as minor or trace minerals (see sample geochemistry). Irregular, easily removable, cm- to dm-size concretionary gypsum aggregates occur locally, although not throughout the section.The abundance of gypsum generally does not exceed trace-mineral levels away from the mentioned enrichments.

In most samples the kaolinite has a poor crystal order based on the diffraction maxima in the region 19.5–22.0°2θ. Because the samples contain varying amounts of quartz, characterization by methods such

https://doi.org/10.1180/claymin.2017.052.3.01 Published online by Cambridge University Press

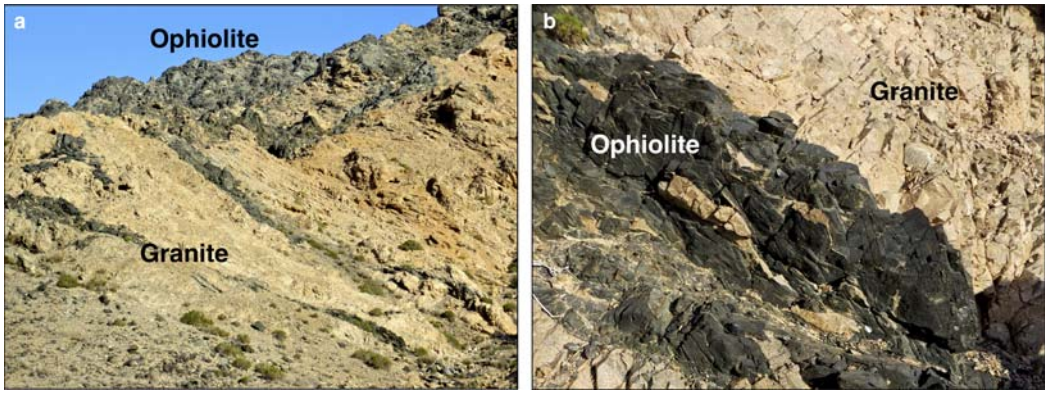

FIG. 6. (a) Granitic dykes and pods (pink) cross-cutting dark ophiolitic rocks; the lens widening towards the left is ~40 m thick in its widest part; (b) close-up of granitic dyke (pink) with relicts of the ophiolitic host rocks (dark); width of view is ~5 m.

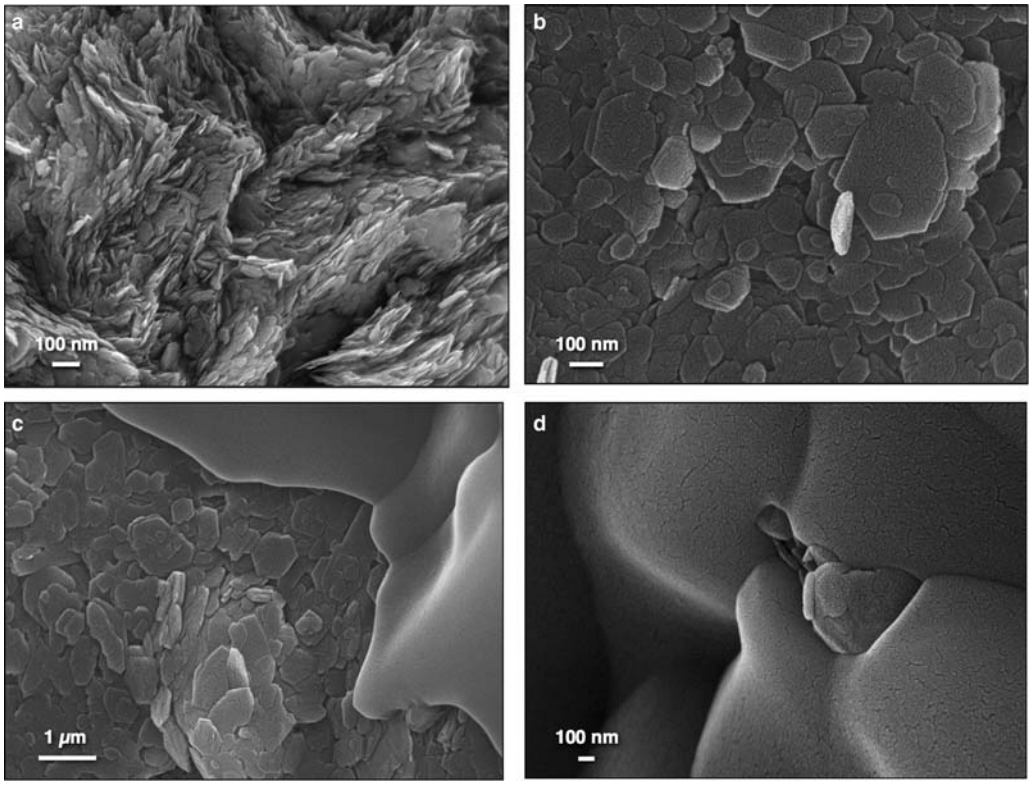

FIG. 7. (a) SEM SE image of strongly undulating texture perpendicular to the bedding occurs throughout the sample; (b) SEM image of the layer's surface, on which euhedral thin platelets cover each other; the typical stacked kaolinite grains are absent; kaolinite surfaces exhibit dehydration-like cracks; (c) SEM SE image showing that, in places, kaolinite layers are covered by an amorphous and almost structureless coating of SiO_2; (d) even at high magnification, the SiO_2 coating remains structureless and only displays fine dehydration-like cracks; a fine kaolinite grain protrudes at the center of the image.

https://doi.org/10.1180/claymin.2017.052.3.01 Published online by Cambridge University Press

TABLE 1. Semi-quantitative mineral composition and kaolinite crystal order, according to Hinckley (1963), of the Masirah samples; for comparison, two different kaolinites were included in the evaluation.

#	Kaolinite[a] (%)	Quartz[a] (%)	Peak development[b]	Accompanying minerals
M1	93.6	6.4	only small (020)	Some natroalunite
M2	86	14	only small (020)	Some natroalunite
M3	76	24	none	Very similar to M8A
M4	78.4	21.6	only small (020)	Similar to M8A
M5	87	–	3 well developed peaks	Goethite (~13%), gypsum (trace mineral)
M8	76.7	23.3	only small (020)	Anatase, Halite
M8A	76	24	only small (020)	Anatase, Gypsum (trace mineral)
Commercial Kaolinite	100	–	3 well developed peaks	none
Kaolinite Mandoos Gossan	100	–	3 well developed peaks	none

[a]Semi-quantitative approach using the main quartz peak at 26.62°2θ.
[b]Kaolinite peak development (≈ crystal order) in the region between 19.5 and 22.0°2θ.

as the Hinckley Index is unreliable (Hinckley, 1963; Aparicio & Galán, 1999). Nevertheless, the size or absence of these peaks clearly reflects limited ordering. Only one of the Masirah clays (M5) plus the control samples (commercial kaolinite and material from the Mandoos gossan in Oman) are well crystallized (Table 1 Fig. 8b). The low structural order of the clay minerals might also have been suggestive of halloysite, which can be an alteration product of mafic rocks (Joussein *et al.*, 2005). However, halloysite was not identified in any of the samples.

The identification under the SEM of what was initially believed to be amorphous SiO_2 coatings/sheets between kaolinite platelets was not confirmed by the XRD traces, which revealed the presence of quartz instead. The XRD trace of the material with the greatest SiO_2 content is shown in Fig. 8c. Opal-A and opal-CT traces from Lynne & Campbell (2004) were superimposed on the Masirah sample together with a quartz trace. There is no correspondence to any of the opal peaks but a rather straight-forward correlation with quartz (with all other quartz peaks as well, which are not displayed). Thus, because no quartz grains were detected in any of the samples examined, all the silica coatings are, in fact, well crystallised quartz. Similar, but much larger-scale quartz grains and patches were found in Omani gossan materials associated with highly acidic mine drainage (in prep.). The mobility and abundance of SiO_2 in this environment inhibited the possible formation of gibbsite by binding all mobile Al to Si during the formation of kaolinite and natroalunite (see below).

Using XRD, a number of minerals (natroalunite, jarosite, natrojarosite and brushite ($Ca(HPO_4)\cdot 2H_2O$)) was identified in the deposit which only form under extremely acidic conditions during gossan formation, in the course of and after the breakdown of sulfide minerals. This acidity and the associated chemical overprinting has more or less affected the entire clay section. Hematite, goethite, gypsum and quartz are remnants of this process although the relatively high mobility of SiO_2 under these conditions is a little-discussed fact (unpublished data) that manifests itself in the coatings.

Mineralogy of the ceramics

The changes to sample M8A after firing at 900 and 1040°C are illustrated in Figure 9. The original kaolinite trace disappeared, leaving a very broad 'bump' while quartz levels are roughly halved suggesting reaction with kaolinite. Small additional peaks in the ceramic material reflect minor amounts of anatase; no firing-induced minerals, such as calcium silicates, were detected because of the composition of the raw material.

Chemical composition

The Masirah clay samples were analysed for their major, minor and trace-element compositions to

https://doi.org/10.1180/claymin.2017.052.3.01 Published online by Cambridge University Press

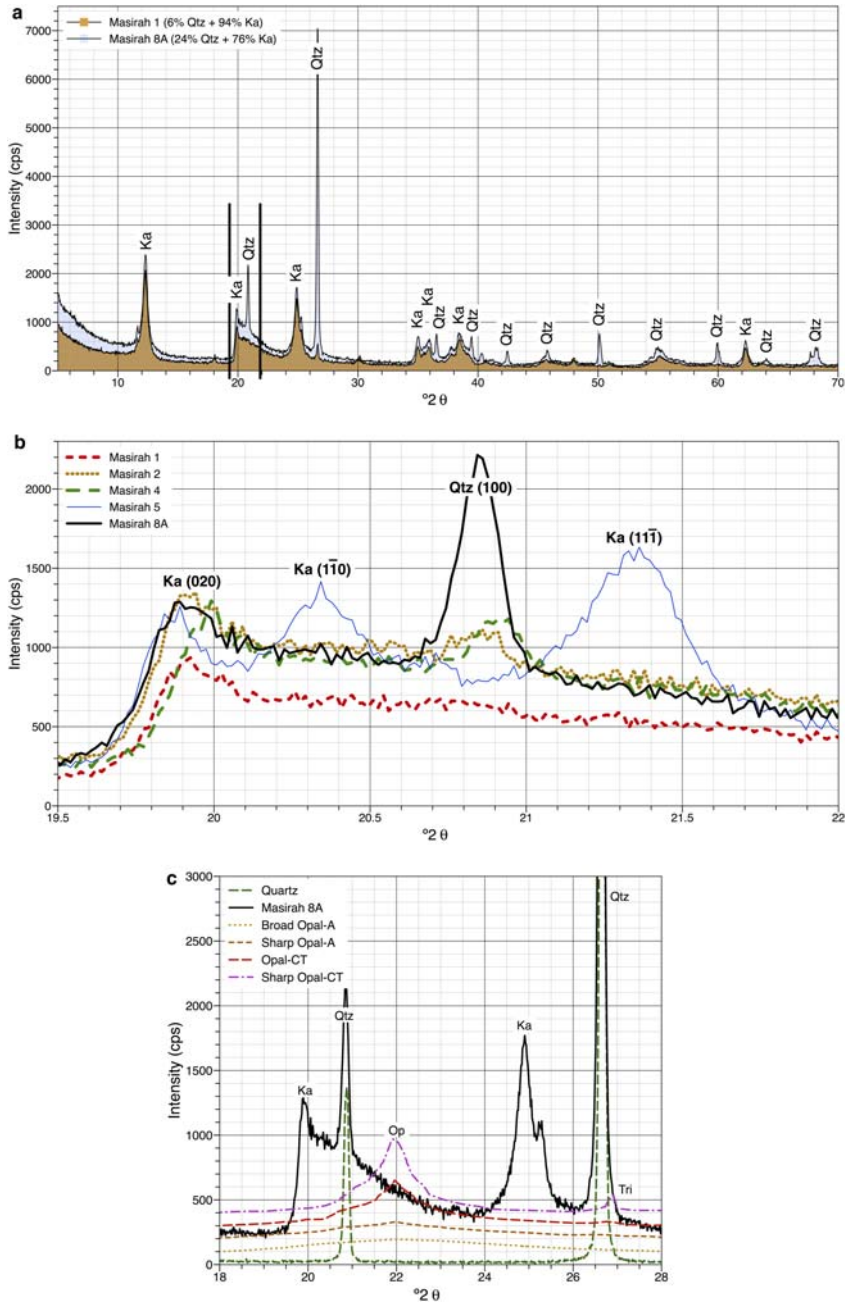

FIG. 8. (a) Comparison of XRD traces of two kaolinites exhibiting the maximum variability of kaolinite (Ka) and quartz (Qtz) concentrations in the Masirah samples; the two vertical bars indicate the range of the peaks shown in detail in Fig. 8b; (b) kaolinite crystal order is generally very poor, with the exception of sample M5; (c) identification of SiO_2 modification by comparing the XRD trace of the natural sample (M8A) with the traces of quartz and different varieties of opal; Ka, kaolinite; Qtz, quartz; Op, opal; Tri, tridymite; the opal and quartz traces are not plotted to scale (intensity) with sample M8A; opal data after Lynne & Campbell (2004).

https://doi.org/10.1180/claymin.2017.052.3.01 Published online by Cambridge University Press

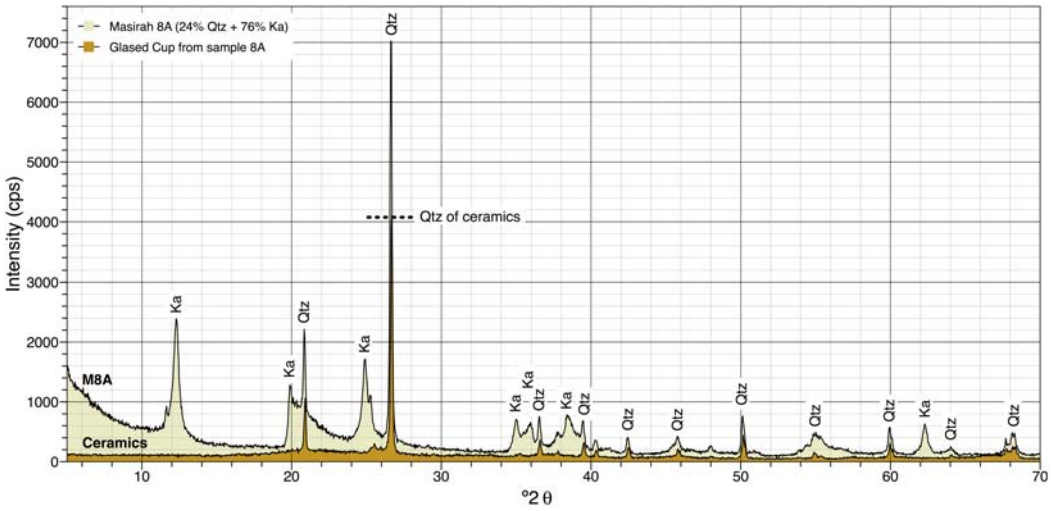

FIG. 9. Comparison of XRD trace of a kaolinite sample from Masirah with the glazed ceramic material made from the same sample (M8A); quartz (Qtz) and kaolinite (Ka) appear in the natural sample, while the clay XRD trace disappears in the fired material and quartz decreases in abundance.

identify components detrimental to the firing of clays (Tables 2, 3). Most samples are relatively free of carbonate contamination with values generally well below 0.5 wt.%, despite the proximity to limestones. The smaller amounts of carbonate (up to a couple of percent) could easily be counterbalanced by further addition of quartz (resulting in the formation of calcium silicate upon firing). Carbonate mostly appears as fine-grained diffuse impregnation in the clays (up to a few hundred μm in size), which would be difficult to remove physically.

The clays also show variable iron concentrations. Raised iron levels are mostly undesirable for high-grade ceramics, because of ochre to red-brown ferric oxide colouration of the ceramics after calcination at high temperature, which reduces the quality of otherwise light-coloured clays. However, with the exception of sample M5, most materials of this site contain much less Fe (Table 2) and only result in a slight discolouration that still renders the clays suitable for local use.

The preparation and successive firing of Masirah clays did not encounter problems from the low halite content of the clays (ceramics would be used mainly by the local craft industry as replacements for imports). Most samples contain <500 ppm Cl^-; some of the chloride was probably washed out during the beneficiation of the raw material. Nevertheless, although not observed in the Masirah clays, greater NaCl abundances influence the liquid limit of the clay (LL decreases with increasing salt levels) and need to be considered in places with increased concentration (Fatahi *et al.*, 2011).

There is no direct evidence for the origin of the kaolin on Masirah. However, because lateritic kaolin may develop from any of the rocks mentioned above, including shales (Schellmann, 1986; McFarlane & Bowden, 1992; Michailidis *et al.*, 1993; Malengreau & Sposito, 1997; Bourman & Ollier, 2002), possible source rocks were evaluated by normalizing their major, minor and trace element abundances against different rocks that are related to the sedimentary and igneous environments of the deposit. The clay should, in any case, have retained chemical indicators for its origin and would display these in normalization plots or discrimination diagrams (*REE* data are not available for the Masirah samples, which were analysed for *LREE*s but were below the detection limit).

The following normalizations were performed (Fig. 10a,b):

- N-MORB (Loucks & Ballard, 2003), to examine the possibility of *in situ* alteration of basalts to kaolinite-rich materials (authors' unpublished findings of high-acidity basalt alteration; see also McAdam *et al.*, 2008); unless eroded, completely replaced or physically displaced, gabbros/basalts normally overlie ultramafic ophiolitic rocks;
- Post-Archaean Average Australian Shales (PAAS; Taylor & McLennan, 1985), assuming

https://doi.org/10.1180/claymin.2017.052.3.01 Published online by Cambridge University Press

Table 2. Major and minor oxides composition of Masirah clay samples.

Sample No.	SiO_2	TiO_2	Al_2O_3	$Fe_2O_3^a$	MgO	CaO	Na_2O	K_2O	P_2O_5	LOI	Total
M1	39.42	1.48	31.68	1.20	0.40	0.29	1.11	0.10	0.02	23.00	**98.70**
M2	39.02	1.54	30.44	1.03	0.61	0.47	1.20	0.12	0.02	24.40	**98.86**
M3	48.31	2.51	24.04	1.15	0.50	0.25	1.25	0.19	0.03	21.00	**99.23**
M4	39.62	1.57	28.28	0.95	0.40	0.26	1.64	0.14	0.03	26.50	**99.39**
M5	38.25	0.25	33.52	5.97	0.10	0.24	1.01	0.05	0.00	18.80	**98.20**
M7	44.40	1.53	10.06	1.75	1.00	12.50	0.50	0.23	0.01	25.40	**97.41**
M8	42.36	2.58	28.79	1.54	0.34	0.16	1.45	0.11	0.02	21.80	**99.17**
M8A	51.83	1.79	25.86	1.49	0.44	0.33	0.80	0.32	0.03	15.90	**98.79**

Concentrations are in wt.%.
[a]Denotes total Fe_2O_3.

Table 3. Trace-element composition of selected Masirah clay samples.

#	Rb	Sr	Ba	Zr	Nb	Th	V	Cr	Ni	Co	Cu	Zn	La	Ce	Nd
M1-1	3	119	–	182	25	9	132	466	67	49	31	21	–	–	–
M3-1	11	69	–	362	43	13	122	99	26	40	14	24	–	–	–
M8-1	5	64	74	186	25	9	120	178	79	–	16	19	66	80	134

Concentrations are in ppm; As, Pb, Pr and U are below detection limit.

a greater transport distance and depositional environments similar to shale source materials; and

- K-Granite from Masirah (Abbotts, 1978) to compare the samples with a potential source rock in the vicinity of the clay deposits.

When comparing the three normalized major- and minor-element patterns (Fig. 10a), the samples display relatively homogenous spider diagrams for the major and minor elements with an undulating shape of the N-MORB, a more even distribution for the PAAS, and a fairly linear distribution for the K-Granite. Not surprisingly, SiO_2 and Al_2O_3 as the main constituents of kaolinite are scarcely changed in the normalizations whereas TiO_2 peaks most in the granite norm. Although MgO seems to be depleted in all norms with the exception of sample M7, it correlates positively with CaO which derives from secondary carbonates; MgO shows depletions for both N-MORB and PAAS, while it appears enriched in the granite norm (this might be seen as an indicator of mafics/ultramafics-derived overprinting). Iron also behaves similarly to MgO, but only showing enrichment in the

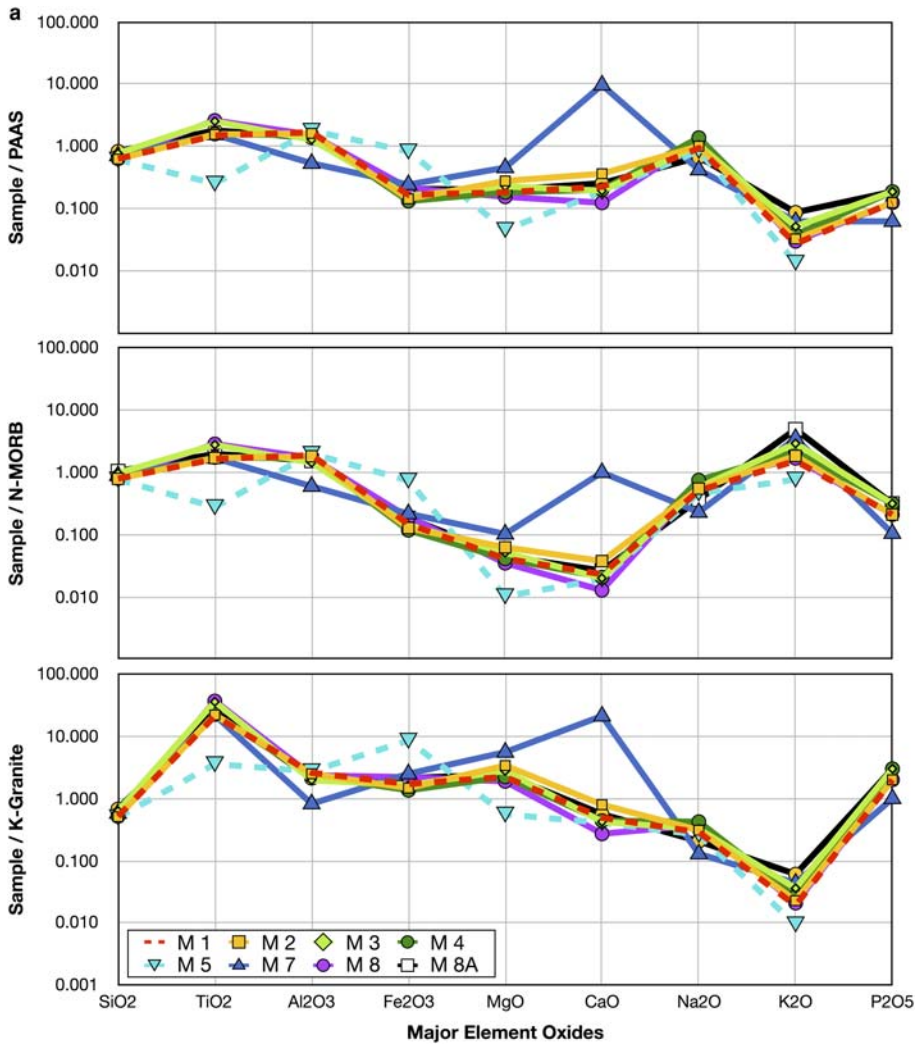

FIG. 10. (a) Comparison of the PAAS-/N-MORB-/K-Granite-normalized major and minor oxide patterns of the Masirah clays; (b) comparison of the PAAS-/N-MORB-/K-Granite-normalized trace-element patterns of the Masirah clays.

https://doi.org/10.1180/claymin.2017.052.3.01 Published online by Cambridge University Press

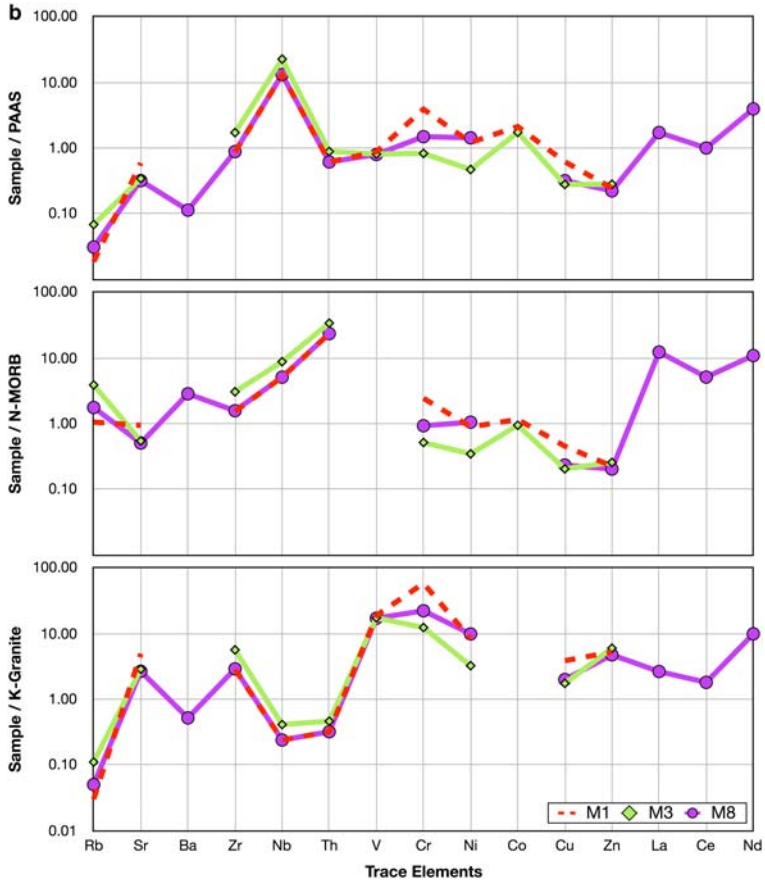

FIG. 10. Continued.

granite norm. Slight Fe_2O_3 impregnations in most of the clays discussed cause colour tints from greenish grey to slightly beige, suggesting some secondary-enrichment effects. Despite low concentrations of fine-grained NaCl as observed under the SEM, in all samples, Na mostly displays depletion in the norm patterns. This is not surprising as Na is highly soluble and easily mobilized. The same applies to potassium, which shows strong depletion in the PAAS and K-Granite norms. However, there is a well-developed positive potassium anomaly for the N-MORB, which is difficult to explain. The last of the major- and minor-element group is P_2O_5 with depletions for N-MORB and PAAS norms, while the small phosphate enrichment seen in the K-Granite pattern seems to reflect the presence of phosphorous in the form of brushite concretions encountered in lower sections of the deposit. Overall, and regardless of the present location of the deposit in relation to a possible source rock, the K-Granite norm pattern seems to best explain this compositional group.

The normalized trace-element patterns (Fig. 10b) differ more in their respective shapes than the diagrams for the major and minor elements. However, this illustrates the fact that there has been a secondary overprint on at least some parts of the deposit from highly acidic fluids of a gossan development below the clay deposit. The addition of further elements from the breakdown of sulfide minerals and the successive interaction with clay components (SiO_2 and Al_2O_3) should have affected the trace elements to a greater degree than the major elements, while those elements that were not or only little changed in abundance by the overprint display the information relating to the clay genesis. Nevertheless, V, Cr, Ni, Cu and Zn display major to minor enrichments in the K-Granite norm, which reflects field observations and analyses that all support the secondary overprint. This view is strongly supported by a

https://doi.org/10.1180/claymin.2017.052.3.01 Published online by Cambridge University Press

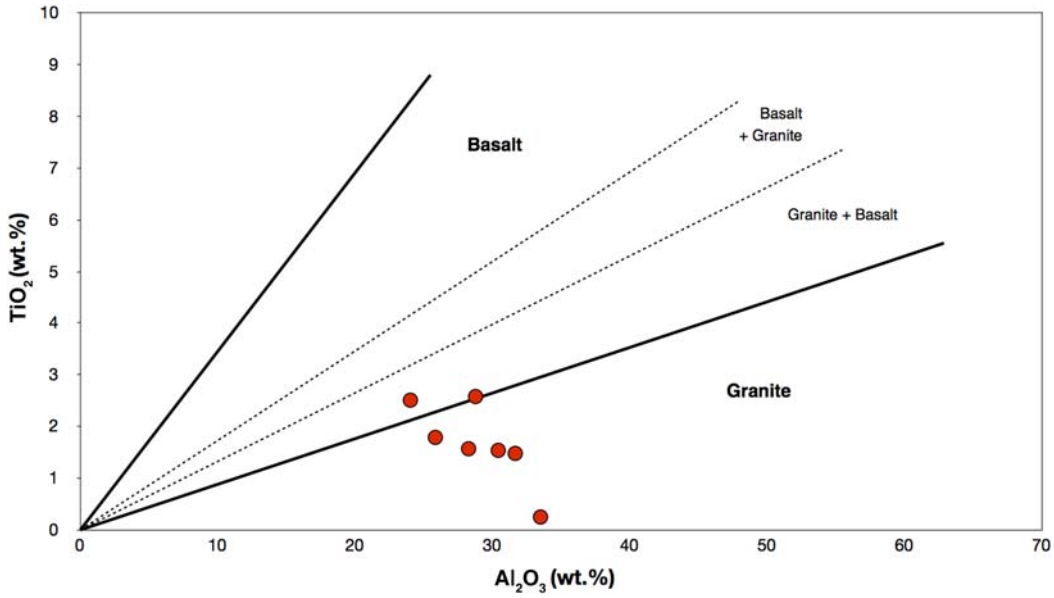

FIG. 11. Discrimination plot for source rocks of kaolinitic clays (after Amajor, 1987).

discrimination diagram by Amajor (1987; Fig. 11), which distinguishes granites and basalts as source rocks of kaolinitic clays on the basis of Al_2O_3 and TiO_2 contents. All samples plot in the granite or granite-basalt fields, distant from the basalt area.

Technological behaviour

The term plasticity refers to changes in the shape of a clay-water mass in a non-elastic, non-reversible manner (Moore, 1965). Industrially, almost all of the clay materials are used in the plastic state and the significant parameters to characterize them are the liquid limit (LL), the plastic limit (PL) and the plasticity index (PI) (Bain & Highley, 1979; Siddiqui *et al.*, 2005). Most data for the Masirah kaolins cluster in the range of modest shrinkage relatively close to the field for optimal moulding and are, thus, suitable for pottery applications (Table 4, Fig. 12).

TABLE 4. Results of plasticity tests for Masirah samples.

Sample No	Liquid Limit, LL (%)	Plastic Limit, PL (%)	Plasticity Index, PI (%)
M1	74	34	40
M2	76	28	48
M3	59	25	34
M4	47	27	20
M5	56	31	25
M6	45	32	13
M7	60	27	31
M8	64	31	33

A quick assessment of the suitability of the respective clay samples for direct firing without the addition of quartz is presented in Fig. 13. The theoretical line for a mixture of kaolin to quartz content (75:25, as required for industrial purposes) cross-cuts the points for samples M3 and M8A, which, according to the semiquantitative data in Table 1, show kaolinite-quartz ratios of 76:24. Minor additions of other minerals were not evaluated but will result in a shift along the line, reflecting a dilution by these minerals; otherwise the samples still suggest an ideal ratio for kaolin and quartz. Deviations from the line imply non-ideal mixtures, which could, for instance, be balanced by adding quartz (all samples above the line). Additional minerals such as carbonates, goethite, halite, *etc*. would also affect the plot positions by shifting the sample to a lower part of the line by means of dilution of both kaolin and quartz. An example is sample M6 which contains >40 wt.% Fe_2O_3 but plots close to the line. Such material would still yield suitable material provided that the admixtures were easily removed.

https://doi.org/10.1180/claymin.2017.052.3.01 Published online by Cambridge University Press

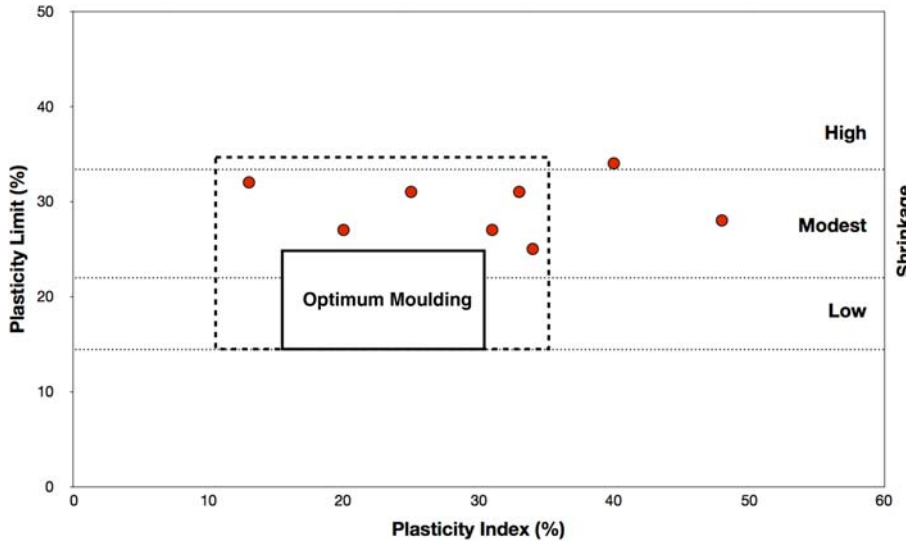

FIG. 12. Representation of the quality of the Masirah kaolinite samples for industrial applications.

DISCUSSION

Genesis of the Masirah clay

The kaolin in Jabal Humr area belongs to a Tertiary sequence unconformably overlying the Masirah ophiolite complex. At this contact, the succession starts with the clay unit, which is covered, in turn, by bryozoan, nodular and nummulitic limestones. At Jabal Humr itself, patchy red ferruginous clayey materials that have been referred to as laterite (Peters *et al.*, 1995; Menkveld-Gfeller & Decrouez, 2004)

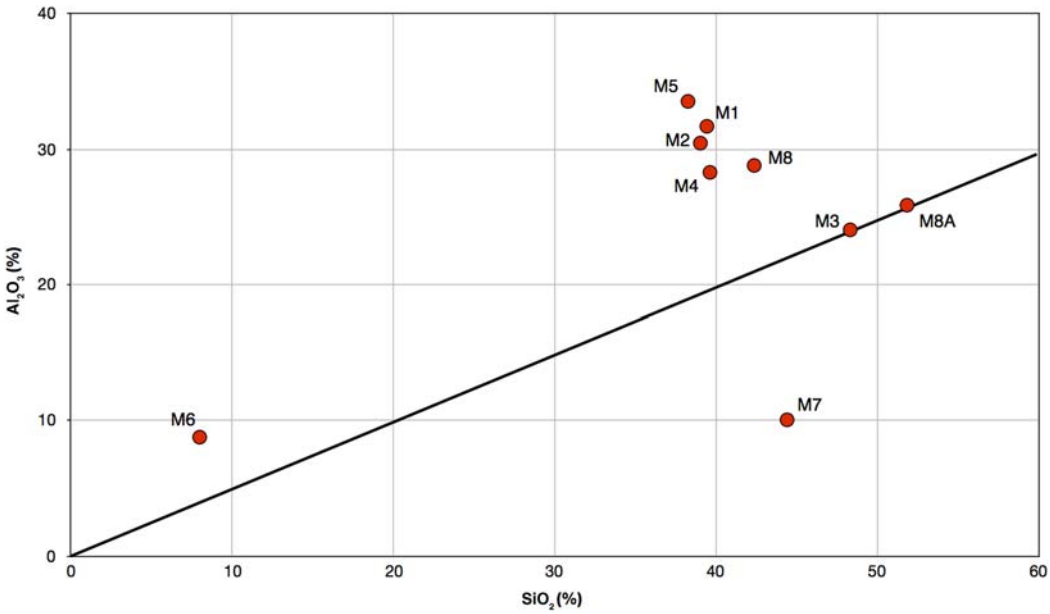

FIG. 13. Correlation of SiO_2 and Al_2O_3 for the collected clay samples; the black line depicts the ratio between ideal mixtures of kaolinite and quartz (75:25). Raw materials plotting close to the line can be fired without further addition of quartz.

https://doi.org/10.1180/claymin.2017.052.3.01 Published online by Cambridge University Press

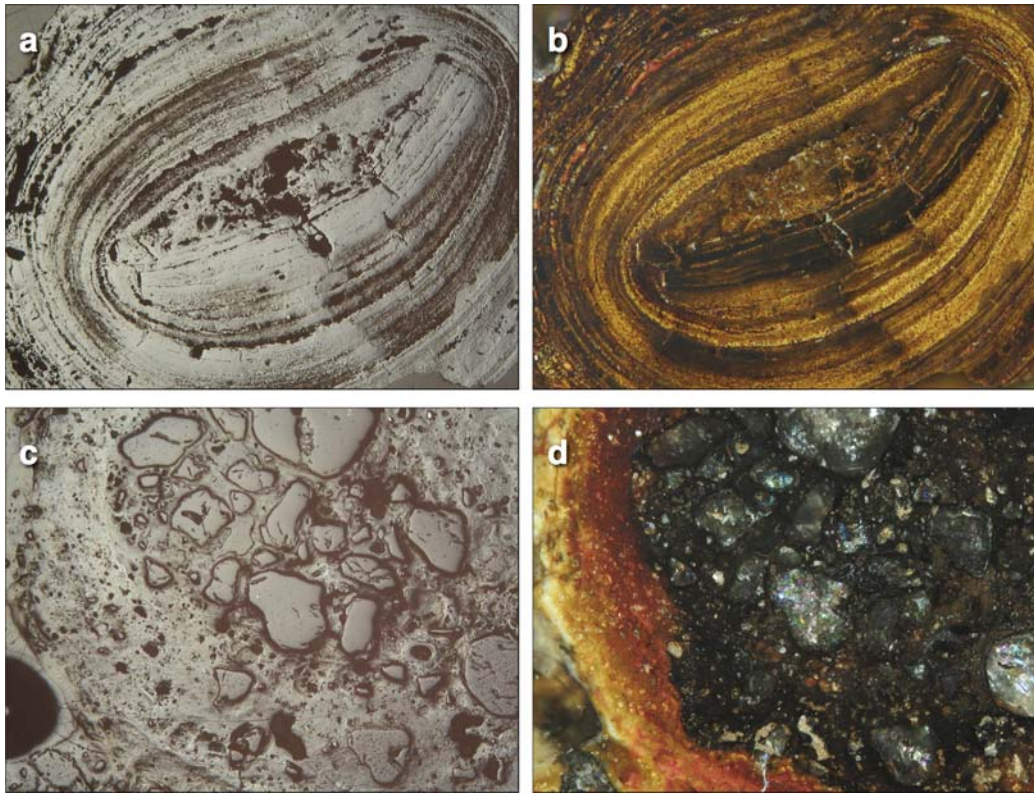

FIG. 14. (a) Polished section of a ferruginous pisolith from Masirah, composed mainly of goethite, shallow-marine origin, viewed under PPL in reflected light; note fine lamination produced by high-energy environment and the large angular nucleus composed of a pisolith fragment; (b) the same grain viewed under XPL, goethite (brown internal reflections) is accompanied by a minor amount of hematite (red internal reflections); (c) polished section of a ferruginous soil spherulith from Groote Eylandt (Northern Territory, Australia), lateritic origin; viewed under PPL in reflected light; note the multiple irregular quartz nuclei enveloped by a very crude lamination produced by low-energy soil creep; (d) the same grain viewed under XPL, goethite (brown to reddish internal reflections), quartz (multi-colour internal reflections), very fine Mn oxide cement (dark). Both grains have the same magnification, the long edge of all photos is 2.8 mm long.

separate the ophiolite from the kaolinite section (*cf.* Fig. 3).

There is no visible evidence for the presence of any lateritic profile in the ~10 m thick clay sequences; the bed is very homogeneous and seems to be undisturbed. A grading into saprolite, which would normally be revealed through mottled and partially bleached red-brown and light beige patches (close association of clays and iron) as well as parent rock relicts, was not observed. Despite the iron staining, most of the clays in the deposit carry insignificant amounts of Fe, and appear slightly cream to greenish white in colour. Another typical feature, the crudely laminated ferruginous spherulitic soils at the top of a lateritic sequence (*cf.* Pracejus *et al.*, 1988), is absent although a very small shallow-marine iron oolite/pisolite deposit above the clay unit (Fig. 14a–d) could and has been misinterpreted as part of a lateritic sequence. However, there are distinct differences between oolites/pisolites and soil spherulites in a polished section under the microscope. Ferruginous pisolites exhibit numerous fine laminae around a nucleus, while soil spherulites are characterized by multiple cemented (sand) grains in the core and very few and coarse laminae surrounding them. These features reflect the completely different kinetic energies during the respective formation (high energy: shallow-marine wave action; low energy: soil creep).

Because some iron enrichment also occurs in direct contact with the overlying limestones, it is necessary to

https://doi.org/10.1180/claymin.2017.052.3.01 Published online by Cambridge University Press

first examine the possibility of kaolin formation through lateritization. Assuming at least some remnants of basaltic/gabbroic materials after moderately strong erosion of the upper ophiolite section on Masirah, lateritic leaching would indeed produce some of the observed minerals, such as hematite, kaolinite and quartz (*e.g.* Taylor *et al.*, 1992; Hill *et al.*, 2000; Greenberger *et al.*, 2012). However, similar weathering profiles and alteration products may also result from lateritization of a serpentinized peridotite such as that present in the Masirah ophiolite (Gaudin *et al.*, 2011). Both types of mafic and ultramafic rocks are thus closely associated with the kaolin and residual iron oxides (Nesbitt &Wilson, 1992). The lack of Mg minerals (Mg derived from ophiolitic rocks) in any of the alteration products is not surprising because Mg^{2+} is very mobile during alteration and normally moves away from its original location; in an evaporitic sequence, magnesium compounds precipitate very late due to their high solubility products (Bąbel & Schreiber, 2014).

When dealing with lateritic sequences, the calculation of weathering indices might provide useful insights into the weathering history of the samples examined (*e.g.* Price &Velbel, 2003). Two different indices have been employed here in order to see if a consistent picture emerges (Table 5): Weathering Index of Parker (WIP; Parker, 1970); Chemical Index of Weathering (CIW; Harnois, 1988).

The two indices yielded contradictory results, showing that the samples are either extremely fresh and unaltered (WIP) or almost completely altered (CIW). All samples except for M7 contain secondary carbonates in fairly low concentrations. Because calculations should include only CaO derived from silicates (Price & Velbel 2003), CaO was excluded from the calculation in a second step and WIP* and CIW* were obtained (Table 5). This procedure smoothed the values as evidenced by the standard deviations, but did not change the overall picture. The authors conclude, therefore, that from the point of view of calculation of weathering indices there is no direct link to a weathering profile in our samples. This view is also supported by field evidence which yielded no indication of rock fragments within the clays, even at the base of the section where a saprolite should be developed, as mentioned above.

None of the findings to date indicate a laterite formation in the Masirah clays. However, location in an ophiolitic setting, where ultramafic, mafic and felsic rocks and sediments occur in close association, the sample normalization performed against mafic (N-MORB), felsic (K-granite from Masirah), and sediments (PAAS) correlated the chemical composition encountered with possible source rocks (*cf.* geochemistry section). Although the normalization, especially that of the K-Granite, shows elevated chromium values (Table 3 Fig. 10b), there is no record of chromite grains in the clay, which contains 100–450 ppm Cr. Nevertheless, an enrichment of this magnitude could even have been derived from mafic rocks within a gossan environment where Cr is mobile and released from the host rocks (in prep.). Had the kaolinite, on the other hand, been derived from lateritization of a dunite (3000–4000 ppm Cr) or wehrlite (500–1,000 ppm Cr), chromium values would have increased to much greater abundances than those observed and chromite

Table 5. Weathering indices after Parker (1970; WIP) and Harnois (1988; CIW).

Sample No.	WIP	WIP[a] – without CaO	CIW	CIW[b] – without CaO
M1	800	759	96	97
M2	917	849	95	96
M3	958	922	94	95
M4	1,131	1,094	94	95
M5	663	628	96	97
M7	2,367	581	44	95
M8	977	954	95	95
M8A	809	762	96	97
Average	1,077.57	818.64	88.62	95.87
Std. dev.	539.30	171.22	18.20	0.98
	fresh: optimum >100 altered: optimum 0		fresh: optimum ≤50 altered: optimum 100	

[a]According to Price & Velbel (2003) only CaO deriving from silicates should be used for index calculation.

https://doi.org/10.1180/claymin.2017.052.3.01 Published online by Cambridge University Press

grains would have survived lateritization. Similarly, there is no account of significant amounts of nickel (Table 3), which would have been an essential marker for lateritization overprinting ultramafic rocks. Thus, there is no indication for *in situ* enrichment from such a sequence, further contradicting a lateritic origin. Comparing the different normalized patterns (Fig. 10a,b), the K-Granite norm produces the most consistent line patterns for major and minor elements (Fig. 11), while the trace elements and the occasional field occurrence of secondary copper minerals point to an input of base metals (unlike the N-MORB and PAAS diagrams), something that is also corroborated by the presence of the argillic alteration minerals, which must have been in association with elevated base-metal levels.

These two latter factors, the metals in conjunction with the secondary sulfates natroalunite, jarosite and natrojarosite plus the phosphate and brushite, indicate a high acidity that might have overprinted the clay unit. However, the pH value necessary for their formation (<4) can only develop in a gossan environment through the oxidation of sulfides, which in turn leads to the formation of sulfuric acid (Chavéz, 2000). Acidic fluids from such a process would predominantly carry SO_4^{2-}, Fe^{2+}, and H_4SiO_4 near the surface of the unit (redox dependent), while other heavy metals would be more mobile lower down within an orebody. Had such fluids reached an existing clay section or, alternatively, mafic rocks (basalts/gabbros), the superposition by the sulfates mentioned would have been a natural consequence, as would a fine-grained quartz precipitate in the alteration products (Al-Mahrouqi *et al.*, 2015; *cf.* Fig. 7c,d). The presence of quartz would also have suppressed the formation of gibbsite, another typical laterite mineral that only forms at extremely low Si concentration (Pracejus, 1990). Thus, an advanced argillic alteration produces the kind of mineral association that was observed in the Masirah clay deposit (Panteleyev & Koyanagi, 1993; McCollom *et al.*, 2013).

Supporting this view is the fact that large (dm-sized) gypsum crystals and even larger gypsum concretions of up to 1 m in diameter were observed in association with the kaolinite units. Mobilization of calcium (Ca^{2+}) from the overlying limestone through interaction with the acidic fluids of a gossan environment below, would precipitate gypsum (gypsum is not stable in a laterite). The limestone dissolution is evidenced in various places by large cavities at its base, although typical karst features such as karren or sinters were not found. In the northern part of the deposit, enormous limestone slabs have simply broken off the top units in massive landslides indicating an extensive mass removal lower down the section. Calcium mobility is also reflected by the development of brushite (providing the Ca for this phosphate) in an acidic surrounding within the clays and near the contact with the underlying ophiolite.

These findings all point to an advanced argillic alteration of igneous rocks and a subsequent overprinting event that affected the clays. However, as in the case of saprolite formation during lateritization, there is no gradational texture or mineralogical/geochemical gradient visible in the field that could be taken as evidence of an *in situ* formation of the deposit. Thus, it is necessary to look for further clues that might reflect the deposit's provenance.

According to Balan *et al.* (2007), a "neoformation" (second generation) of kaolinite is often characterized by a much lower crystal order. The Masirah clays are characterized by poorly crystalline kaolinite at the base of the deposit, while a variety with higher crystal order occurs further upwards in the section (sample M5 in Fig. 3 and Table 1). Thus, the highly acidic fluids, which forced the argillic alteration, may also have led to the re-crystallization of pre-existing kaolinite. In parallel, this overprinting process might have caused physicochemical changes within the fluids that caused the deposition of finest quartz layers covering the re-crystallized kaolinite, apparently moving across the solubility product of quartz which is lower than that of amorphous silica/opal (Gunnarsson & Arnórsson, 2000). Quartz precipitation is common in Omani gossan environments where secondary quartz often accompanies many other alteration products, while opal is absent.

If this latter scenario is adopted then there remains the question of the protolith. As the clays clearly don't show large iron concentrations, which would be expected in context with mafic or ultramafic rocks, the source rock might have significantly less iron, implying more felsic igneous rocks, such as granites (Evans, 1993; Montes *et al.*, 2002). However, an *in situ* emplacement through granite alteration is unlikely because accessory minerals that would have been typical for the respective origin are almost completely lacking (except for minor amounts of anatase), which suggests that the kaolinite should have been transported and re-deposited.

Nevertheless, the most likely protoliths for the Masirah clays are the K-granites which crop out in the immediate vicinity of the Tertiary rocks in the Jabal Humr area (~1 km SW of the kaolin location), forming

https://doi.org/10.1180/claymin.2017.052.3.01 Published online by Cambridge University Press

up to 200 m-thick veins, sheets and irregular pods up to 40 m wide (Figs 5 and 6a,b). Exposed over an area of some 4 km^2, the granites intrude the Masirah ophiolite (Abbotts, 1978; Smewing *et al.*, 1991; Peters *et al.*, 1995). Compositionally, the pink to cream-grey coloured Masirah granites have an average modal composition of 41.9% quartz, 34.5% orthoclase, 21.6% plagioclase and 2% biotite, while the textures range from coarse granular to mylonitic (Abbotts, 1978). Depending on the characteristics of the inferred felsic parent material, the chemical composition and mineralogy of the alteration mineral, such as kaolinite or illite, also varies (Keller, 1978). Assuming a K-granite as the parent rock, the possibility of an initial alteration to illite exists (Sequeira Braga *et al.*, 2002) because of the availability of potassium in both K-feldspar and biotite, although there is no evidence for any illite. Moreover, neither does the Masirah granite contain significant amounts of sericite/muscovite from which illite often forms (Elsass *et al.*, 1997). However, had illite been produced in a first step, a conversion to kaolinite and a mobilization/loss of potassium from the system would have occurred under a lower-temperature hydrothermal regime (Robertson & Eggleton, 1991), because illite would be metastable with regards to the feldspar-kaolinite equilibrium (<200°C; Sass *et al.*, 1987). Because there is no evidence for such an additional overprint, it will no longer be considered; instead it is suggested that a direct alteration to kaolinite is most likely.

Industrial uses for the Masirah clay

The Masirah clay has good plasticity, optimum amounts of SiO_2 and Al_2O_3, small amounts of TiO_2, and relatively small amounts of Fe_2O_3 (Table 2). Therefore it is suitable for the local ceramics industry. Although the Fe_2O_3 content, in general, slightly exceeds 1%, which may affect the brightness/whiteness of the pottery, the ceramics are still within the acceptable limit (Prasad *et al.*, 1991). Apart from the ceramics industry, Masirah clay might also meet paper-filling and -coating specifications (Prasad *et al.*, 1991) with few excess-minerals contents. However, colour measurement would be necessary to assess suitability for paper applications.

The Masirah clay was tested experimentally at the Bahla Pottery factory by heating at 940 and 1040°C, to assess its suitability for the ceramics industry. Cracks developed in the ceramic articles upon cooling indicating the weak strength of the product. The kaolin was then mixed with 25% of fine-grained quartz and was left to dry for 24 h before being heated at 1040°C. The addition of quartz substantially improved the quality of the mixture, especially in the samples with original quartz content significantly <25% required for fabrication of ceramics; the finished products had considerably greater material strength. Mixing clays with common tempers such as quartz, shell fragments, calcite and bones has been common practice in the manufacture of traditional ceramics (Rye, 1976; Rice, 1987; Orton, 2009). The addition of quartz to the clay in volume fractions >20% improves the toughness of the fired product at 950°C (Kilikoglou *et al.*, 1995; Kilikoglou & Vekinis, 1998). Although Allegretta *et al.* (2015) did not observe significant changes in the strength of kaolin-quartz mixtures after heating at 750°C, the present study shows substantial improvement of the ceramics after addition of quartz temper and firing at 1040°C. Industrial processing, however, should minimize quartz addition to an overall concentration of 25% to reduce costs.

CONCLUDING REMARKS

Our field observations together with mineralogical and geochemical data suggest that the Masirah kaolin deposits passed through the following development stages:

- Alteration of exhumed granitic bodies (contained in the ophiolite) led to the formation of kaolinite.
- Kaolinite was eroded and deposited in a coastal basin/lagoon.
- A transgression then flooded the basin, leading to a partial erosion of upper parts of the clay unit due to the higher-energy environment, as evidenced by a small oolitic/pisolitic ironstone deposit between the present top of the kaolinite and the overlying limestone.
- This was followed by the deposition of a limestone cap in shallow waters.
- The successive regression exposed the rocks to the atmosphere and accelerated their erosion.
- Due to the exposition to atmospheric conditions, the oxidation of sulfide minerals contained in a small sulfide orebody (slags from ancient copper mining exist in the vicinity of the clays) of the underlying ophiolite overprinted the clays with highly acid fluids ($pH < 2$ and formation of argillic alteration minerals) and also destroyed all evidence of marine (micro-)fossils.

The Masirah clays are generally suitable for commercial use and benefit from the presence of very fine-grained quartz. The commercial ceramics mixtures contain ~25% quartz while the Masirah clays consist

https://doi.org/10.1180/claymin.2017.052.3.01 Published online by Cambridge University Press

of between 6 and 24% quartz. The natural clays require small amounts of quartz temper for the firing process, thus reducing the costs in terms of the preparation of ceramics. Occasional iron enrichments might cause a light brownish staining to the ceramics, but do not diminish the overall quality of the products.

ACKNOWLEDGEMENTS

This paper has benefitted greatly from an exchange of ideas with Prof. George E. Christidis (Technical University of Crete, School of Mineral Resources Engineering, 73100 Chania, Greece) and from suggestions made by the reviewers. The project was part of a larger investigation on clay deposits in Oman (SQU Project No. CR/SCI/ETHS/13/03) and was funded by the Bahla Pottery Factory and the Public Authority for Craft Industry (PACI) through the Industrial Innovation Centre (IIC; No. P-2011-008). Dr Lorna Cork's (Innovation Consultant) continuous support during this study is greatly appreciated. Drs El-Said El-Shafey (Dept. of Chemistry, SQU) and Ahmed Al-Busaidi (Dept of Soil Science, SQU) helped with various analyses. Mr Rashid Al-Hinai (PACI) is thanked for his help during field trips. Mr Saif Al-Mamari and Mrs Samira Al-Kharusi (CAARU, SQU) are thanked for their lab support.

REFERENCES

Abbotts I.L. (1978) High-potassium granites in the Masirah ophiolite of Oman. *Geological Magazine*, **115**, 415–425.

Ahmed I., Al-Khirbash S., Pracejus B., El-Shafey S., Al-Busaidi A., Al-Aamri M., Al-Hinai R. & Cork L. (2014) *Exploration and prospection of white clay (kaolinite) deposits in the Sultanate of Oman and its potential for industrial use for the Bahla pottery factory*. Final report to the Public Authority for Craft Industry and the Industrial Innovation Center, Sultan Qaboos University, Muscat. 106 pp.

Al-Mahrouqi K., Al-Kindi O. & Pracejus B. (2015) Gossan alteration products – key to environmentally friendly mine remediation? Pp. 88–90 in: *Proceedings of the The Seventh Environmental Symposium of German-Arab Scientific Forum for Environmental Studies*. Sultan Qaboos University, Muscat, Oman, Sultan Qaboos University.

Allegretta I., Eramo G., Pinto D. & Kilikoglou V. (2015) Strength of kaolinite-based ceramics: Comparison between limestone- and quartz-tempered bodies. *Applied Clay Science*, **116–117**, 220–230.

Amajor L.C. (1987) Major and trace elements geochemistry of Albian and Turonian shales from the southern Benue Trough, Nigeria. *Journal of African Earth Science*, **6**, 633–461.

Aparicio P. & Galán E. (1999) Mineralogical interference on kaolinite crystallinity index measurements. *Clays and Clay Minerals*, **47**, 12–27.

Bąbel M. & Schreiber B.C. (2014) Geochemistry of evaporites and evolution of seawater. Treatise on Geochemistry (2nd Edition): Sediments. *Diagenesis and Sedimentary Rocks*, **9**, 483–560.

Bain J.A. & Highley D.E. (1979) Regional appraisal of clay resources – a challenge to the clay mineralogist. *Developments in Sedimentology*, **27**, 437–446.

Balan E., Fritsch E., Allard T. & Calas G. (2007) Inheritance vs. neoformation of kaolinite during lateritic soil formation: A case study in the middle Amazon basin. *Clays and Clay Minerals*, **55**, 253–259.

Béchennec F., De Métour J., Platel J.P. & Roger J. (1993) *Geological Map of the Sultanate of Oman (GIS Version, 1:250,000)*. Ministry of Petroleum and Minerals, Directorate General of Minerals, Muscat.

Bourman R.P. & Ollier C.D. (2002) A critique of the Schellmann definition and classification of laterite. *Catena*, **47**, 117–131.

Chavéz Jr, W.X. (2000) Supergene oxidation of copper deposits: Zoning and distribution copper oxide minerals. *SEG Newsletter*, **41**, 9–21.

Elsass F., Środoń J. & Robert M. (1997) Illite-smectite alteration and accompanying reactions in a Pennsylvanian underclay studied by TEM. *Clays and Clay Minerals*, **45**, 390–403.

Essalhi M., Sizaret S., Barbanson L., Chen Y., Lagroix F., Demory F., Nieto J.M., Sáez R. & Capitán M.A. (2011) A case study of the internal structures of gossans and weathering processes in the Iberian pyrite belt using magnetic fabrics and paleomagnetic dating. *Mineralium Deposita*, **46**, 981–999.

Evans A.M. (1993) *Ore Geology and Industrial Minerals - an Introduction*. 3rd Edition. Blackwell Science Ltd, Oxford, UK, 389 pp.

Fatahi B., Khabbaz H. & Basack S. (2011) Effects of salinity and sand content on liquid limit and hydraulic conductivity. *Australian Geomechanics*, **46**, 67–76.

Galley A.G., Hannington M.D. & Jonasson I.R. (2007) Volcanogenic massive sulphide deposits. Pp. 141–161 in: *Mineral Deposits of Canada: A Synthesis of Major Deposit Types, District Metallogeny, the Evolution of Geological Provinces, and Exploration Methods*, vol. 5 (W.D. Goodfellow, editor). Geological Association of Canada, Mineral Deposits Devision, Special publication St. Johns, Canada.

Gaudin A., Dehouck E. & Mangold N. (2011) Evidence for weathering on early Mars from a comparison with terrestrial weathering profiles. *Icarus*, **216**, 257–268.

Gnos E. & Perrin M. (1996) Formation and evolution of the Masirah ophiolite constrained by paleomagnetic study of volcanic rocks. *Tectonophysics*, **253**, 53–64.

Greenberger R.N., Mustard J.F., Kumar P.S., Dyar M.D., Breves E.A. & Sklute E.C. (2012) Low temperature aqueous alteration of basalt: Mineral assemblages of

https://doi.org/10.1180/claymin.2017.052.3.01 Published online by Cambridge University Press

deccan basalts and implications for Mars. *Journal of Geophysical Research*, **117**, 21.

Gunnarsson I. & Arnórsson S. (2000) Amorphous silica solubility and the thermodynamic properties of $H_4SiO°_4$ in the range of 0° to 350°C at P_{sat}. *Geochimica et Cosmochimica Acta*, **64**, 2295–2307.

Hannington M.D., Galley A.G., Herzig P.M. & Petersen S. (1998) Comparison of the TAG mound and stockwork complex with Cyprus-type massive sulfide deposits. *Proceedings of the Ocean Drilling Program, Scientific Results*, **Leg 158**, 389–415.

Harnois L. (1988) The CIW index: A new chemical index of weathering. *Sedimentary Geology*, **55**, 319–322.

Hill I.G., Worden R.H. & Meighan I.G. (2000) Geochemical evolution of a palaeolaterite: The interbasaltic formation, Northern Ireland. *Chemical Geology*, **166**, 65–84.

Hinckley D.N. (1963) Variability in "crystallinity" values among the kaolin deposits of the coastal plain of Georgia and South Carolina. *Clays and Clay Minerals*, **11**, 229–235.

Immenhauser A. (1996) Cretaceous sedimentary rocks on the Masirah ophiolite (Sultanate of Oman): Evidence for an unusual bathymetric history. *Journal of the Geological Society London*, **153**, 539–551.

Joussein E., Petit S., Churchman J., Theng B., Righi D. & Delvaux B. (2005) Halloysite clay minerals – a review. *Clay Minerals*, **40**, 383–426.

Keller W.D. (1978) Kaolinization of feldspar as displayed in scanning electron micrographs. *Geology*, **6**, 184–188.

Kilikoglou V. & Vekinis G. (1998) Finite element analysis for failure prediction of archaeological pottery. In: *Proceedings of the 31st International Symposium on Archaeometry*, Budapest, Hungary.

Kilikoglou V., Vekinis G. & Maniatis Y. (1995) Toughening of ceramic earthenwares by quartz inclusions: An ancient art revisited. *Acta Metallurgica et Materialia*, **43**, 59–65.

Loucks R.R. & Ballard J.R. (2003) *Petrochemical characteristics, petrogenesis and tectonic habits of gold-ore-forming arc magmas*. Unpublished report for industry-sponsored research project: Predictive Guides to Copper and Gold Mineralization at Circum-Pacific Convergent Plate Margins, 69 pp.

Lynne B.Y. & Campbell K.A. (2004) Morphologic and mineralogic transitions from opal-A to opal-CT in low-temperature siliceous sinter diagenesis, Taupo volcanic zone, New Zealand. *Journal of Sedimentary Research*, **74**, 561–579.

Malengreau N. & Sposito G. (1997) Short-time dissolution mechanisms of kaolinite tropical soils. *Geochimica et Cosmochimica Acta*, **61**, 4297–4307.

Marquer D., Peter T.J. & Gnos E. (1995) A new structural interpretation for the emplacement of the Masirah ophiolites (Oman): A main Paleocene intra-oceanic thrust. *Geodinamica Acta*, **8**, 13–19.

Marquer D., Mercolli I. & Peters T. (1998) Early cretaceous intra-oceanic rifting in the proto-Indian ocean recorded in the Masirah ophiolite, Sultanate of Oman. *Tectonophysics*, **292**, 1–16.

McAdam A.C., Zolotov M.Y., Mironenko M.V. & Sharp T.G. (2008) Formation of silica by low-temperature acid alteration of Martian rocks: Physical-chemical constraints. *Journal of Geophysical Research, Planets*, **113**, 8.

McCollom T.M., Robbins M., Moskowitz B., Berquó T.S., Jöns N. & Hynek B.M. (2013) Experimental study of acid-sulfate alteration of basalt and implications for sulfate deposits on Mars. *Journal of Geophysical Research: Planets*, **118**, 577–614.

McFarlane M.J. & Bowden D.J. (1992) Mobilization of aluminium in the weathering profiles of the African surface in Malawi. *Earth Surface Processes and Landforms*, **17**, 789–805.

Menkveld-Gfeller U. & Decrouez D. (2004) The Paleogene of Masirah island (Sultanate of Oman). *Neues Jahrbuch der Geologie Palãontologie*, **234**, 311–333.

Michailidis K., Tsirambides A., & Tsamantouridis P. (1993) Kaolin weathering crusts on gabbroic rocks at Griva, Macedonia, Greece. *Applied Clay Science*, **8**, 19–36.

Montes C.R., Melfi A.J., Carvalho A., Vieira-Coelho A.C. & Formoso M.L.L. (2002) Genesis, mineralogy and geochemistry of kaolin deposits of the Jari river, Amapá state, Brazil. *Clays and Clay Minerals*, **50**, 494–503.

Moore F. (1965) *Rheology of Ceramic Systems*. Pp. 51–57. McLaren and Sons, London.

Nesbitt H.W. & Wilson R.E. (1992) Recent chemical weathering of basalts. *American Journal of Science*, **292**, 740–777.

Orton C. (2009) Four pots good, two pots bad: Exploring the limits of quantification in the study of archaeological ceramics. Pp. 65–73 in: *Proceedings of the New Perspectives on Ancient Pottery*. University of Amsterdam, The Netherlands.

Panteleyev A. & Koyanagi V.M. (1993) Advanced argillic alteration in bonanza volcanic rocks, northern Vancouver Island – Transitions between porphyry copper and epithermal environments. *Geological Fieldwork (1992)*, **1**, 287–293.

Parker A. (1970) An index of weathering for silicate rocks. *Geological Magazine*, **107**, 501–504.

Peters T.J. & Mercolli I. (1998) Extremely thin oceanic crust in the proto-Indian ocean: Evidence from the Masirah ophiolite, Sultanate of Oman. *Journal of Geophysical Research*, **103**, 677–689.

Peters T.J., Immenhauser A., Mercolli I. & Meyer J. (1995) *Geological map of Masirah North and Masirah South with Explanatory Notes*. Sheet K768, Directorate General of Minerals, Oman Ministry of Petroleum and Minerals.

Pracejus B. (1990) Groote Eylandt manganese norm – New application of mineral normalization techniques

https://doi.org/10.1180/claymin.2017.052.3.01 Published online by Cambridge University Press

on supergene alteration products. Pp. 3–16 in: *Sediment-hosted Mineral Deposits, Special Publications of the International Association of Sedimentology*, vol. **11** (J. Parnell, Y. Lianjun & C. Changming, editors). Blackwell, Oxford, London, Edinburgh, Boston.

Pracejus B., Bolton B.R. & Frakes L.A. (1988) Nature and development of supergene manganese deposits, Groote Eylandt, Northern Territory, Australia. *Ore Geology Reviews*, **4**, 71–99.

Prasad M.S., Reid K.J. & Murray H.H. (1991) Kaolin: Processing, properties and applications. *Applied Clay Science*, **6**, 87–119.

Price J.R. & Velbel M.A. (2003) Chemical weathering indices applied to weathering profiles developed on heterogeneous felsic metamorphic parent rocks. *Chemical Geology*, **202**, 397–416.

Rice P.M. (1987) *Pottery Analysis*. 2nd Edition. University of Chicago Press, Chicago, Illinois, USA, 592 pp.

Robertson I.D. & Eggleton R.A. (1991) Weathering of granitic muscovite to kaolinite and halloysite and of plagioclase-derived kaolinite to halloysite. *Clays and Clay Minerals*, **39**, 113–126.

Rye O.S. (1976) Keeping your temper under control: Materials and the manufacture of Papuan pottery. *Archaeology and Physical Anthropology in Oceania*, **11**, 106–137.

Sass B.M., Rosenberg P.E. & Kittrick J.A. (1987) The stability of illite/smectite during diagenesis: An experimental study. *Geochimica et Cosmochimica Acta*, **51**, 2103–2115.

Schellmann W. (1986) A new definition of laterite. *Geological Survey of India Memoirs*, **120**.

Sequeira Braga M.A., Paquet H. & Begonha A. (2002) Weathering of granites in a temperate climate (NW Portugal): Granitic saprolites and arenization. *Catena*, **49**, 41–56.

Siddiqui M.A., Ahmed Z. & Saleemi A.A. (2005) Evaluation of Swat kaolin deposits of Pakistan for industrial uses. *Applied Clay Science*, **29**, 55–72.

Smewing J.D., Abbotts I.L., Dunne L.A. & Rex D.C. (1991) Formation and emplacement ages of the Masirah ophiolite, Sultanate of Oman. *Geology*, **19**, 453–456.

Taylor S.R. & McLennan S.M. (1985) *The Continental Crust: Its Composition and Evolution*. Blackwell, Malden, Massachusetts, USA, 132 pp.

Taylor G., Eggleton R.A., Holzhauer C.C., Maconachie L. A., Gordon M., Brown M.C. & McQueen K.G. (1992) Cool climate lateritic and bauxitic weathering. *Journal of Geology*, **100**, 669–677.

https://doi.org/10.1180/claymin.2017.052.3.01 Published online by Cambridge University Press